Nanoscale

Accepted Manuscript

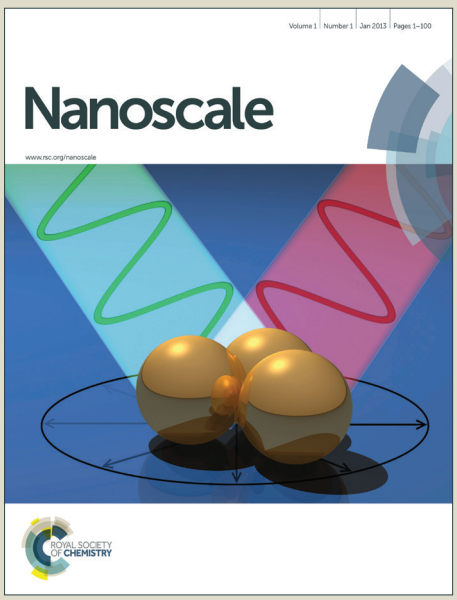

ROYAL SOCIETY OF CHEMISTRY

www.rsc.org/nanoscale

Journal Name

RSCPublishing

COMMUNICATION

Vertical Segregation in the Self-assembly of Nanoparticles at Liquid/Air Interface

Cite this: DOI: 10.1039/x0xx00000x

Yanming Liu,† Yang Liu,† Peng Tao, Wen Shang, Chengyi Song* and Tao Deng*

Received 00th January 2012,
Accepted 00th January 2012

DOI: 10.1039/x0xx00000x

www.rsc.org/

Vertical segregation was induced by the size-dependent charge neutralization during the one-step interfacial self-assembly of colloidal gold nanoparticles with bimodal size distribution. This self-assembly approach also can assemble particles with tunable compositions into layered films.

Interfacial self-assembly of nanoparticles is critical both to the fundamental understanding of assembly process and also to the fabrication of functional thin films.[1-6]The study of self-assembly processes most of time involves nanoparticles with single sizes.[7-22]Assembly of nanoparticles with mixed sizes, however, will offer additional freedom in building films with size-segregated structures, which may provide further control in the functions of the films fabricated.[23-25]There are previous efforts in studying the size-segregation in the interfacial self-assembly of charge stabilized nanoparticles with mixed sizes.[25-31] In those studies, only lateral segregation of nanoparticle with different sizes was observed. For example, Yamaki et al. reported the lateral segregation, which was due to the lateral capillary force, of polystyrene nanoparticles with different sizes when the droplets of mixed particles dried on the surface of mercury.[30] Murphy et al. observed the lateral segregation, which was due to the depletion force, of the small nanorods from the large spherical nanoparticles during the drying of the solutions containing such nanorods and spherical nanoparticles.[5, 25] Recently Chen et al. presented the theoretical explanation of the in-plane lateral size segregation process and attributed the separation to the hydrodynamic and capillary forces.[31]

The work reported in this paper presents our observation of a new one-step interfacial self-assembly process that could separate the nanoparticles with mixed sizes along the direction normal to the liquid/air interface (vertical segregation) rather than parallel to the liquid/air interface (lateral segregation). To the best of our knowledge, our finding is the first report of the vertical segregation of particles with different sizes during the one-step self-assembly process. This observation of vertical-segregation will expand the current scope of interfacial self-assembly, and add another possibility in engineering the microstructures of assembled thin films.

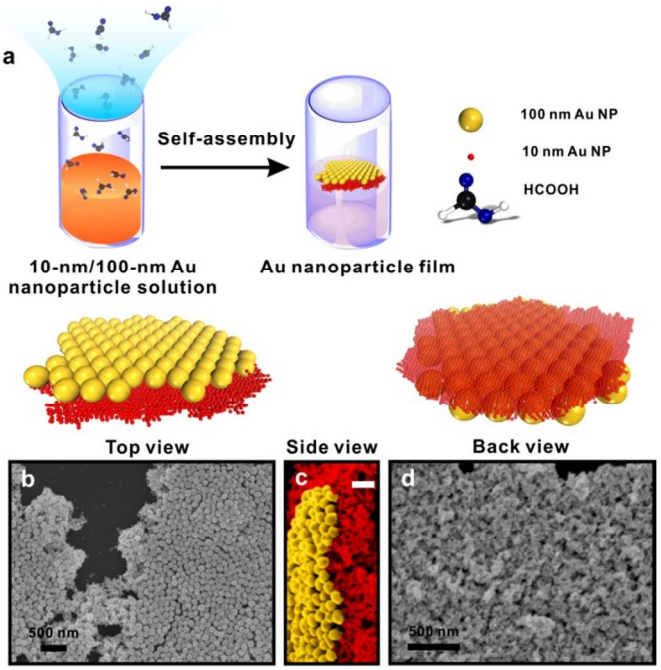

Fig. 1.(a) Preparationof size-segregated double-layered Au NP film via the mixture of 100-nm and 10-nm colloidal Au NP solutions incubating in the presence of formic acid. (b) Top view, (c) side view, (d) back view SEM images of 10 nm/100 nm size-segregated double layered NP film. The middle is a false-color SEM image with upper side of the film facing left (The scale bar is 200 nm.)

In this work, we observed the vertical segregation in the self-assembly of charge stabilized gold (Au) nanoparticles (NPs). There have been reports of interfacial assembly of charge stabilized Au NPs at the liquid/liquid interface or liquid/air

interface through the addition of ethanol or strong electrolyte such as KCl.[10, 16, 18] The work in this report utilized the diffusion of vapor of a weak electrolyte, formic acid, to achieve better control in decreasing the surface charge density of the Au NPs than the processes involving strong electrolytes.[21] The vapor diffusion in the solution also generated a proton gradient that helped move the Au NPs into the liquid/air interface in a controlled fashion. In a typical assembly experiment with the Au NPs of the same sizes (see the Supporting Information for details), a shining film appeared at the water/air interface after overnight exposure to the formic acid (Fig.S4).[21] When the assembly solution containing the mixture of 100-nm and 10-nm citrate capped colloidal Au NPs (concentration of large NPs: ~5.17×10^{10}/ml; concentration of small NPs: ~5.55×10^{12}/ml; see the Supporting Information for the details in the synthesis and characterization of the Au NPs), surprisingly, the vertically size-segregated film formed at the water/air interface, as evidenced by SEM analysis (Fig.1b-d and Fig.S5). Fig.1a shows the scheme of the size-segregated film forming process for the Au NPs solution with bimodal size distribution. When characterizing with the top surface of the segregated film facing up, the SEM shows that the large Au NPs were not mixed with the small Au NPs. They instead mostly sit on top of the layer of small NPs (Fig.1b). When characterizing with the bottom surface of the segregated film facing up, the SEM reveals that the bottom surface was primarily formed by the clusters of small NPs, which blank the view of the large NPs underneath. Considering the small number ratio of 100-nm NPs to 10-nm NPs (1:100), it was rather striking to see such a clear contrast of segregation. Close examination of the side-view SEM image indicated the segregation of the large particles from the small particles in the out-of-plane direction. During SEM sample preparation, trace amount of solution was also attached to the Si substrate and dried in air. To make sure the size segregated double-layer film did not form during SEM sample preparation, the same solution of mixed large and small NPs was also drop-casted onto a Si wafer and dried in air. In this case, only random NP aggregates on the substrate were observed (Fig. S6).

Fig.2 shows the detailed growth process for the vertical segregation of Au NPs with mixed sizes during the film formation process. At the early stage, islands of large NPs occurred at the water/air interface first (Fig. 2a and Fig. S7). After the formation of large NP film, small NPs started to deposit onto the large NP layer during the subsequent assembly process (Fig. 2b, 2c and Fig. S7). As the assembly continued, the small NP film grew denser and completely covered the large NP film (Fig. 2d and Fig. S7). Fig. 2e schematically illustrates the assembly steps that correspond to the SEM images in Figs. 2a-2d.

Continuous monitoring of the optical absorption spectra of the NP solutions during the assembly provides useful insight of the possible mechanism of the formation of the size-segregated double-layer Au NP film. Fig. 3 shows the optical absorption spectra of the solutions that contained 10-nm Au NPs (Fig. 3a), 100-nm Au NPs (Fig. 3b), and mixture of 10-nm and 100-nm Au NPs (Fig. 3c). The time interval for the spectrum collection was 30 mins. As shown in Fig. 3a, the absorption intensity gradually decreased over the course of time. After 210 mins, obvious UV-Vis signal still occurred at 513 nm, indicating that more than half of small Au NPs still remained in the solution (Fig. S8, S9). Differently, the absorption intensity of large NP solution rapidly dropped until it reached zero after 180 mins, which implied almost no large NPs left in the solution (Fig. 3b and Fig. S8, S9). From the absorption spectra of the solution of mixed NPs (Fig. 3c), there was a strong UV-Vis signal because of the superposition of optical absorption from both the small and large NPs solution. The UV-Vis intensity dramatically decreased and the peak blue-shifted to the absorption position of the small NPs (513 nm) after 150 mins. Such shift revealed

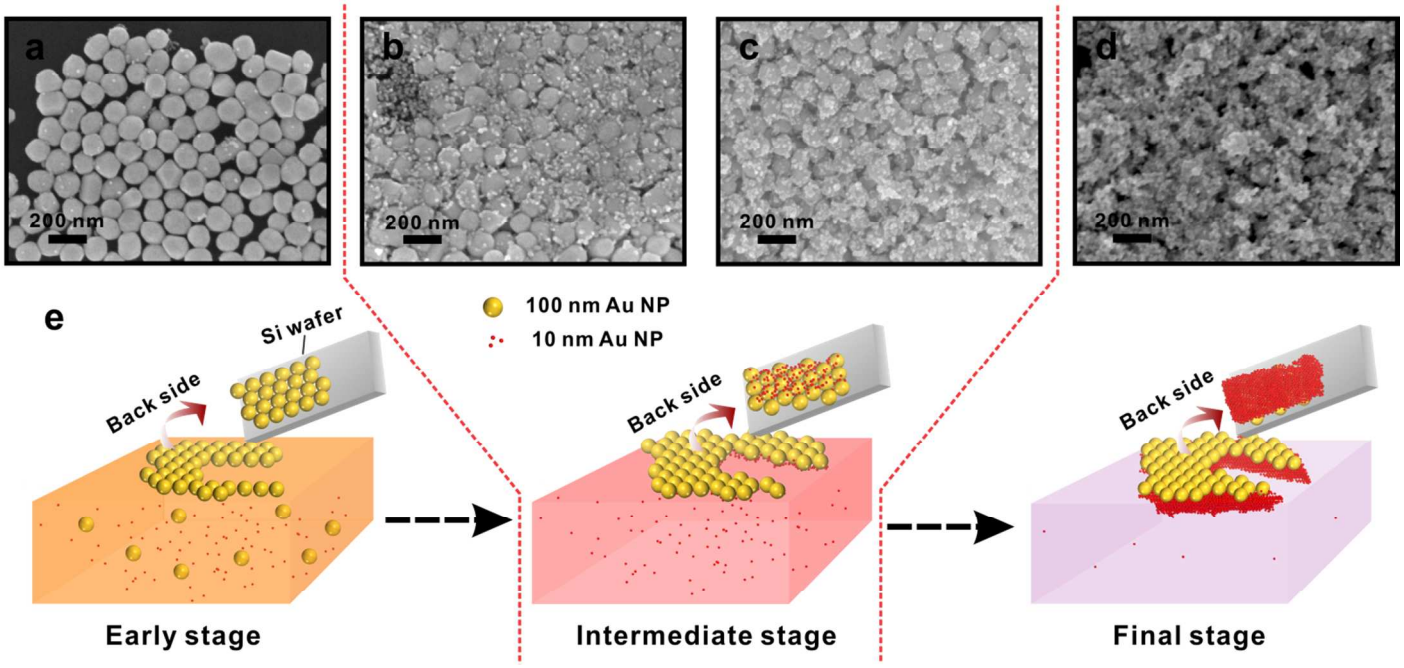

Fig. 2.(a-d) SEM images for the growth process of 10 nm/100 nm size-segregated double layered NP film. (e) Schematic illustration of formation process for size-segregated double layered Au NP films.

that there were almost no large NPs left in solution. Additionally, the peak intensity of the absorption spectrum ($\mathbf{I_2}$ in Fig. 3c) at 150 mins seemed to match with the peak intensity of the absorption spectrum of the solution contained only small NPs at 30 mins ($\mathbf{I_1}$ at Fig. 3a). Apparently, there was a significant decrease in the assembly speed of small NPs in the presence of large NPs in the solution after exposure to the vapor of formic acid. These results confirmed the suppression of the trapping/assembly of small NPs by the large NPs as observed in the SEM analysis (Figs.2a-2d). The absorption spectrum of mixed NPs continued to decrease in intensity after 150 mins, indicating the subsequent assembly of the small NPs at the interface (Fig. 3c and Fig. S8, S9).

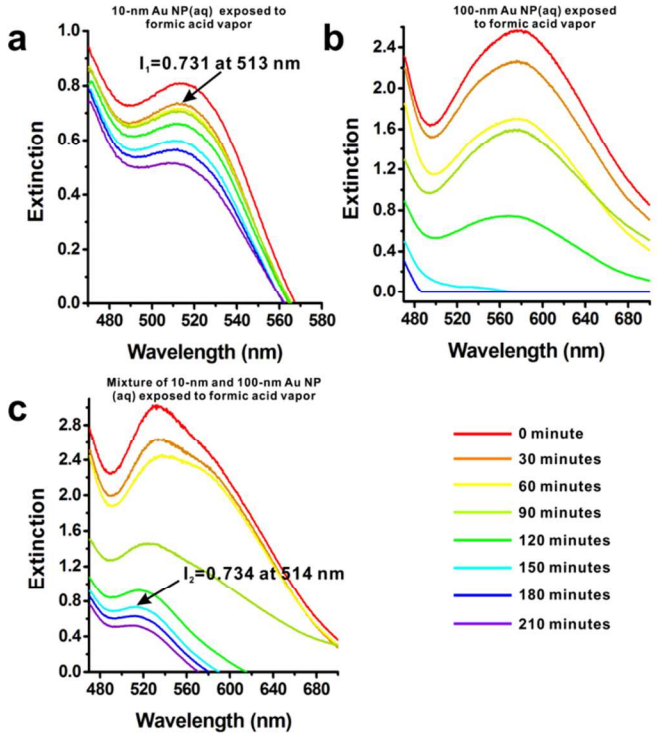

Fig. 3.UV-Vis spectra of solutions containing 10-nm (a), 100-nm (b) and mixture of 10-nm and 100-nm (c) citrate capped Au NPs. The solutions were incubated in the presence of formic acid vapor for 210 mins. The spectra were taken at the time interval of 30 mins. The concentrations of 10-nm Au NPs were the same for both sample 3a and sample 3c; the concentrations of 100-nm Au NPs were the same for both sample 3b and sample 3c.

On the basis of both SEM and optical spectra, following is the proposed process for the vertical segregation of Au NPs at the water/air interface. In the stable solution of charge stabilized colloidal NPs, due to the repulsive electrostatic interaction between the water/air interface and the charge stabilized NPs within the solution, there exists a large energy barrier for the NPs to overcome to be trapped at the interface.[18, 32] During the assembly process studied in this work, the vapour of formic acid filled the desiccator after the evaporation and it also diffused into the solution of colloidal Au NP through the water/air interface. The formic acid dissociated in the aqueous solution and generated hydrogen ions. The hydrogen ions then protonated the citrate groups attached at the surface of the Au NPs and thus reduced the charge density at the NP surfaces. As more charges became neutralized on the NP surfaces, electrostatic repulsion between the particles and the water-air interface decreased. Such decrease helped lower the barrier for the particles to move to the water/air interface.[18, 32] To further prove our hypothesis, we measured the zeta potential of 10-nm Au NPs (aq) in the presence of formic acid vapor at 0 hour, 2 hours, and 6 hours. The zeta potential peak moved from -45.6 mV to -0.82 mV, which implied that the negative surface charges had been balanced by H^+ cations (Figure S10).The surface charge density of the large citrate capped NPs was less than that of the small citrate capped NPs (10-nm Au NPs: -45.6mV;100-nm Au NPs: -20.6mV) (Figure S10). As the vapor of formic acid diffused into the solution, the large NPs became destabilized faster than the small NPs, and they were trapped first at the water/air interface. Once trapped at the interface, the particles helped lower the overall interface energy.[18, 32]

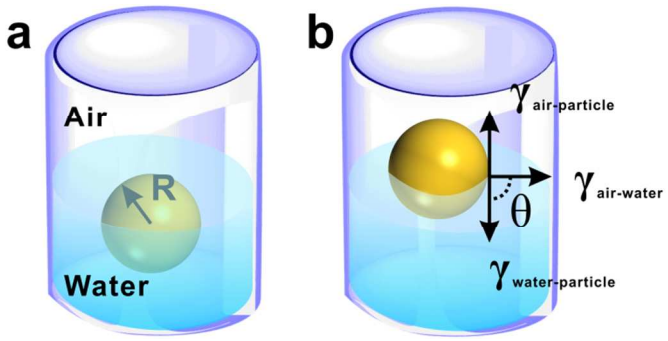

Fig. 4. (a) NPs dispersed in water; (b) NPs trapped at the air-water interface

As shown in Fig. 4, when the NP moves from inside the water to the air/water interface, there is a change of interfacial energy due to the replacement of portion of the air/water interface by the NP. The energy trap of nanoparticles can be determined by the following equation:[33]

$$\mathbf{E_{trap} = \gamma_{air/water} \pi R^2 (1 - \cos\theta)^2} \quad (1)$$

where $\mathbf{E_{trap}}$ is the the overall energy needed (energy trap) to move the particle back from interface to water, **R** is the radius of particles, $\gamma_{air/water}$ is the interfacial surface tension between air and water, and **θ** is the contact angle of individual particles at the water/air interface. Due to the surface line tension of the relatively small particle sizes we used in this study (~10-nm-100-nm), the contact angle at the three phase contact line was estimated to be close to 90° when these particles were trapped at the interface (see the Supporting Information for detailed discussion).[15] The calculated energy trap at the water/air interface can be as large as several hundred $\mathbf{k_BT}$ ($\mathbf{k_B}$ is the Boltzmann constant; **T** is the temperature), and large NPs in general have larger energy trap than small NPs (see the Supporting Information).

After the trapping of the large NPs at the interface, the charge redistributes to the bottom half of the NPs, with dipoles pointing down towards the solvation zone close to the bottom surface of the NPs.[18, 32] Such dipoles not only promote the

dispersion interaction between the large NPs trapped at the interface, but also attract more large NPs inside solution to the bottom of the trapped NPs. The newly attached NPs can move along the first layer to the perimeter of the domain for the growth of the domain.[17] If the domain is too large for an individual NP to move to the perimeter, the newly attached NPs can also stick under the domain to form the second layer of NPs. During this assembly process of large NPs, there is still enough charge on the surface of small NPs, and the charge-induced repulsion not only slows down the trapping of small NPs to the water/air interface, but also prevents the attachment of small NPs to the large NPs. As large NPs deplete due to the assembly at the water/air interface, the charge density of small NPs is further reduced by formic acid. The dipole-dipole interaction between neutralized small and large NPs within the assembled film becomes larger than the electrostatic repulsion. At this stage, the small NPs thus start to attach underneath the large NPs film and grow into a dense 2nd layer primarily consisting of small NPs. Besides the dipole-dipole interaction, there might be other possible forces, for example, hydrogen bonding between–COOH groups anchored on the small and large NPs, that helps the assembly between Au NPs.

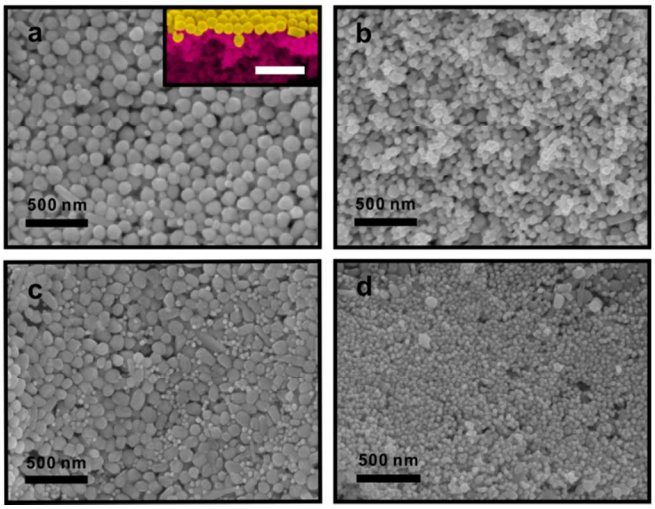

Fig. 5. (a) Top view and (b) back view SEM images of 50-nm Au NP /100-nm Au NP size-segregated double layered NP film. The inset image is side view false-color SEM image of 50-nm/100-nm layered structure. Scale bar is 500 nm. (c) Top view and (d) back view SEM images of 30-nm Au NP /90-nm Ag NP size-segregated double layered NP film.

This work also explored the tuning and tailoring of the structural metrics of vertically segregated double-layer NP film (i.e. NP size and composition). In fact, the assembly using solution containing the mixture of 50-nm Au NP solution (NP size=53.1 ± 4.8 nm; zeta potential: -26.1mV) with 100-nm Au NP solution also resulted in a relatively good vertical size-segregation (Fig.5a-b and Fig. S11). To expand the compositional scope of this approach, the solution with mixture of Au NPs and Ag NPs was also used in the one-step self-assembly process. As synthesized 90-nm colloidal Ag NPs (NP size=91.3 ± 13.7 nm; zeta potential: -25.2mV) have smaller charge density and larger particle size than 30-nm colloidal Au NPs (NP size=33.0 ± 3.8 nm; zeta potential: -30.3mV). The mixture of these Ag NPs and Au NPs would thus possibly lead to the size/composition-segregated double-layer NP film. SEM images reveal that indeed Ag NPs formed a layer first at interface and Au NP layer grew underneath the Ag NP layer (Fig.5c-d and Fig.S12). These above results further prove the speculation that the separated trapping of NPs at the interface, which is related to the gradual reduction of surface charge density, helps the vertical segregation process. If there is enough differentiation of the speed of charge neutralization, it will result in the trapping of NPs at different time and the vertical segregation.

Conclusions

This report presents the first observation of vertical segregation of nanoparticles with mixed sizes during one-step interfacial assembly process. This finding offers opportunity in engineering the structure and composition vertically for the thin film of nanoparticles generated in the interfacial assembly. The controlled assembly process also provides a possible approach in separating particles that have different responding speeds in surface charge neutralization. Such separation was evidenced by the UV-Vis spectroscope study of the assembly solution with NPs of mixed sizes in the present work. The vertical segregation observed might also enable the vertical manipulation of thin film properties, such as the optical and electronic properties. Such vertical property manipulation, however, requires the precise control of the micro/nanostructures of the segregated films, such as the porosity, thickness, and interface between the segregated layers. Substantial effort is still needed to achieve the above controls but the results reported in this work help open the door to develop enabling approaches for applications that involve vertical engineering of thin films of nanoparticles.

Acknowledgements

This work was supported by National Natural Science Foundation of China (Grant No: 91333115), Natural Science Foundation of Shanghai (Grant No: 13ZR1421500 and 14ZR1423300), start-up fund of university of Shanghai Jiao Tong University (Grant No: AF0500045), the postdoctoral international exchange program and the Zhi-Yuan Endowed fund from Shanghai Jiao Tong University. The authors also want to thank Dr. Lin He and Dr. Wei Li for their support and valuable discussions. The authors thank Instrumental Analysis Center of Shanghai Jiao Tong University for access to TEM and SEM.

Notes and references

State Key Laboratory of Metal Matrix Composites, School of Materials Science andEngineering, Shanghai Jiao Tong University,Shanghai 200240, P. R. China.
Email: dengtao@sjtu.edu.cn; chengyi2013@sjtu.edu.cn
†Yanming Liu and Yang Liu equally contributed to this paper.
Electronic Supplementary Information (ESI) available: Experimental procedures and fig. S1-S13. See DOI: 10.1039/b000000x/

1. L. Hu, M. Chen, X. Fang and L. Wu, *Chem. Soc. Rev.*, 2012, **41**, 1350-1362.
2. K. Ariga, Y. Yamauchi, T. Mori and J. P. Hill, *Adv. Mater.*, 2013, **25**, 6477-6512.
3. K. Sakakibara, J. P. Hill and K. Ariga, *Small*, 2011, **7**, 1287-1287.
4. Z. Niu, J. He, T. P. Russell and Q. Wang, *Angew. Chem. Int. Ed.*, 2010, **49**, 10052-10066.
5. K. J. M. Bishop, C. E. Wilmer, S. Soh and B. A. Grzybowski, *Small*, 2009, **5**, 1600-1630.
6. J. Zhang, Y. Li, X. Zhang and B. Yang, *Adv. Mater.*, 2010, **22**, 4249-4269.
7. S. Srivastava, D. Nykypanchuk, M. Fukuto, J. D. Halverson, A. V. Tkachenko, K. G. Yager and O. Gang, *J. Amer. Chem. Soc.*, 2014, **136**, 8323-8332.
8. H. Wu, H. Li, Y. Zhai, X. Xu and Y. Jin, *Adv. Mater.*, 2012, **24**, 1594-1597.
9. H. Xia, Y. Ran, H. Li, X. Tao and D. Wang, *J. Mater. Chem. A*, 2013, **1**, 4678-4684.
10. L. Xu, G. Han, J. Hu, Y. He, J. Pan, Y. Li and J. Xiang,*Phys. Chem. Chem. Phys.*, 2009, **11**, 6490-6497.
11. H.-J. Tsai and Y.-L. Lee, *Soft Matter*, 2009, **5**, 2962-2970.
12. H. Xia and D. Wang, *Adv. Mater.*, 2008, **20**, 4253-4256.
13. T. Ming, X. Kou, H. Chen, T. Wang, H.-L.Tam, K.-W.Cheah, J.-Y. Chen and J. Wang, *Angew. Chem. Int. Ed.*, 2008, **47**, 9685-9690.
14. Y.-K. Park, S.-H.Yoo and S. Park, *Langmuir*, 2007, **23**, 10505-10510.
15. F. Reincke, W. K. Kegel, H. Zhang, M. Nolte, D. Wang, D. Vanmaekelbergh and H. Mohwald, *Phys. Chem. Chem. Phys.*, 2006, **8**, 3828-3835.
16. Y.-J. Li, W.-J.Huang and S.-G. Sun, *Angew. Chem. Int. Ed.,* 2006, **45**, 2537-2539.
17. T. P. Bigioni, X.-M. Lin, T. T. Nguyen, E. I. Corwin, T. A. Witten and H. M. Jaeger, *Nat. Mater.*, 2006, **5**, 265-270.
18. F. Reincke, S. G. Hickey, W. K. Kegel and D. Vanmaekelbergh, *Angew. Chem. Int. Ed.*, 2004, **43**, 458-462.
19. H. Duan, D. Wang, D. G. Kurth and H. Möhwald, *Angew. Chem. Int. Ed.*, 2004, **43**, 5639-5642.
20. E. Rabani, D. R. Reichman, P. L. Geissler and L. E. Brus, *Nature*, 2003, **426**, 271-274.
21. Y.-R. Zhang, Y.-Z.Xu, Y. Xia, W. Huang, F.-A.Liu, Y.-C.Yang and Z.-L. Li, *J. Colloid Interface Sci.*, 2011, **359**, 536-541.
22. H. Wu, H. He, Y. Zhai, H. Li, J. Lai and Y. Jin, *Nanoscale*, 2012, **4**, 6974-6980.
23. J. Wang, D. Wang, N. S. Sobal, M. Giersig, M. Jiang and H. Möhwald, *Angew. Chem. Int. Ed.*, 2006, **45**, 7963-7966.
24. B. Wang, M. Wang, H. Zhang, N. S. Sobal, W. Tong, C. Gao, Y. Wang, M. Giersig, D. Wang and H. Mohwald,*Phys. Chem. Chem. Phys.*, 2007, **9**, 6313-6318.
25. T. K. Sau and C. J. Murphy, *Langmuir*, 2005, **21**, 2923-2929.
26. P. C. Ohara, D. V. Leff, J. R. Heath and W. M. Gelbart, *Phys. Rev. Lett.*, 1995, **75**, 3466-3469.
27. C. J. Kiely, J. Fink, M. Brust, D. Bethell and D. J. Schiffrin, *Nature*, 1998, **396**, 444-446.
28. Y. Liu, X.-M. Lin, Y. Sun and T. Rajh, *J. Amer. Chem. Soc.*, 2013, **135**, 3764-3767.
29. C. G. Sztrum and E. Rabani, *Adv. Mater.*, 2006, **18**, 565-571.
30. M. Yamaki, J. Higo and K. Nagayama, *Langmuir*, 1995, **11**, 2975-2978.
31. S. Chen, Y. Chen, H. Ohashi, Z. Zeng and G. Liang, *Int. J. Mod Phys C*, 2013, **24**, 1340002.
32. P. Pieranski, *Phys. Rev. Lett.*, 1980, **45**, 569-572.
33. B. P. Binks, *Curr. Opin. Colloid Interface Sci.,* 2002, **7**, 21-41.